Eclética Química
ISSN: 0100-4670
ISSN: 1678-4618
ecletica@journal.iq.unesp.br
Universidade Estadual Paulista Júlio de Mesquita Filho
Brasil

Fonsêca, Mateus Cottorello; Marasco Júnior, César Augusto; Dias, Diógenes dos Santos; da Silva, João Pedro; Lamarca, Rafaela Silva; Ribeiro, Clóvis Augusto; Pires, Lorena Oliveira; Gomes, Paulo Clairmont Feitosa de Lima

Sugarcane bagasse biochar pellets for removal of caffeine, norfloxacin, and ciprofloxacin in aqueous samples

Eclética Química, vol. 47, núm. 2, 2022, pp. 82-96
Universidade Estadual Paulista Júlio de Mesquita Filho
Araraquara, Brasil

DOI: https://doi.org/10.26850/1678-4618eqj.v47.2.2022.p82-96

Disponible en: https://www.redalyc.org/articulo.oa?id=42970797005

Eclética Química Journal

Original article

revista.iq.unesp.br

| Vol. 47 | n. 2 | 2022 |

Sugarcane bagasse biochar pellets for removal of caffeine, norfloxacin, and ciprofloxacin in aqueous samples

Mateus Cottorello Fonsêca[1], César Augusto Marasco Júnior[1], Diógenes dos Santos Dias[2], João Pedro da Silva[1], Rafaela Silva Lamarca[1], Clóvis Augusto Ribeiro[2], Lorena Oliveira Pires[2], Paulo Clairmont Feitosa de Lima Gomes[1+]

1. São Paulo State University, National Institute for Alternative Technologies of Detection, Toxicological Evaluation and Removal of Micropollutants and Radioactives, Araraquara, Brazil.
2. São Paulo State University, Institute of Chemistry, Araraquara, Brazil.

+Corresponding author: Paulo Clairmont F. de Lima Gomes, **Phone:** +55 16 33019613 **Email address:** paulo.clairmont@unesp.br

ARTICLE INFO

Article history:
Received: September 17, 2021
Accepted: March 04, 2022
Published: April 01, 2022

Section Editor: Assis Vicente Benedetti

Keywords:
1. torrefaction
2. adsorbent
3. emerging contaminants
4. wastewater
5. removal

ABSTRACT: This work investigates the physicochemical properties of a biochar obtained from sugarcane bagasse by torrefaction at four different temperatures (260, 270, 280, and 290 °C), without chemical or physical activation. The biochar was characterized by thermogravimetric and proximate analysis, Fourier transform infrared spectroscopy (FTIR), scanning electron microscopy, together with measurements of point of zero charge, pH, elemental composition, and surface area. Evaluation regarding the efficiency of the biochar employed as an adsorbent for the removal of caffeine, ciprofloxacin, and norfloxacin in wastewater samples. The assays were performed in batch vessels filled with lab-made sewage spiked with caffeine at 5.00 μg L^{-1} and with ciprofloxacin and norfloxacin at 10.0 μg L^{-1}. These compounds were studied separately. The thermogravimetry data demonstrated that increasing the torrefaction temperature led to generation of a greater amount of fixed carbon, as well as loss of volatile materials and removal of non-condensable compounds. This was corroborated by the FTIR analyses, where a higher temperature led to higher intensity of bands corresponding to methyl, methylene, and C=C bonds. The biochar produced at 280 °C presented the best stability, with adsorption efficiencies for removal from the lab-made sewage of 91% (norfloxacin), 81% (ciprofloxacin), and 58% (caffeine).

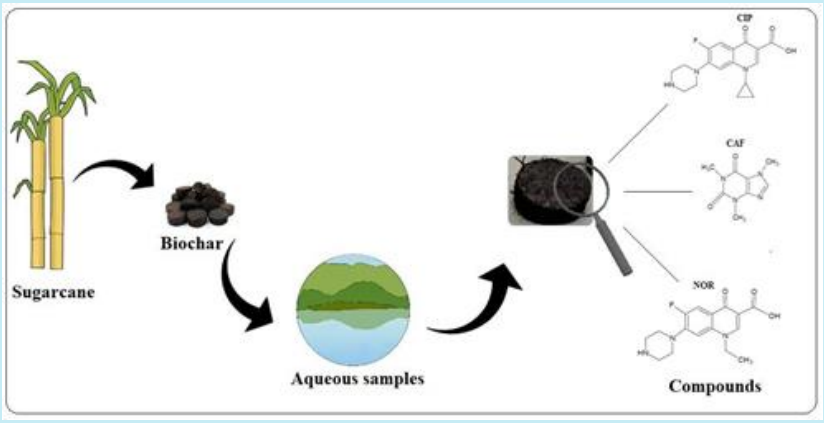

Eclética Química Journal, vol. 47, n. 2, 2022, 82-96
ISSN: 1678-4618
DOI: 10.26850/1678-4618eqj.v47.2.2022.p82-96

1. Introduction

Biochar is a solid material obtained by the thermochemical conversion of biomass in an oxygen-restricted environment (International Biochar Initiative, 2015). The characteristics of biochar include porous structure, large specific surface area, mechanical resistance, acid and alkaline corrosion resistance, ion exchange capacity, and diverse chemical functionalities. These properties provide biochar with many different possible uses, including environmental applications such as the removal of organic and inorganic contaminants, water purification, and soil remediation and fertilization (L. Li *et al.*, 2019; Oliveira *et al.*, 2017; Wang *et al.*, 2017).

Inyang and Dickenson (2015) reported higher adsorption efficiency of organic contaminants on biochar, compared to activated carbon. The presence of biochar in soil provides benefits such as reduced nutrient leaching, promotion of crop growth, and reduced methane (CH_4) emissions. Biochar can incorporate fertilizers and nutrients for controlled release, reducing nutrient shortages in the soil (Liu *et al.*, 2019). Another important point to be highlighted is that compared to biochar, the cost of activated carbon is estimated to be 20 times higher, due to high energy consumption and low productivity (Mohanty *et al.*, 2018).

Caffeine (CAF), norfloxacin (NOR), and ciprofloxacin (CIP) are in the class of emerging contaminants. CAF is highlighted because it is a marker of anthropogenic activity and is present in wastewater at concentration levels from μg L^{-1} to ng L^{-1} (Marasco Júnior *et al.*, 2019). CIP and NOR, which are frequently found in wastewater samples at μg L^{-1} concentration level, are broad-spectrum antibiotics of the fluoroquinolone class, widely applied in human and veterinary medicine. In 2019, quinolones were present in more of the 21 million prescriptions in the USA (Buehrle *et al.*, 2021).

Table 1 presents the physicochemical characteristics of the CAF, CIP and NOR.

Table 1. Physicochemical properties of the studied compounds.

Compound	CAF	CIP	NOR
Chemical structure	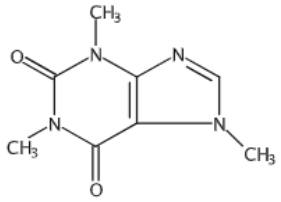	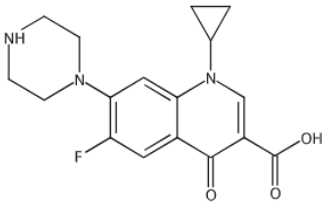	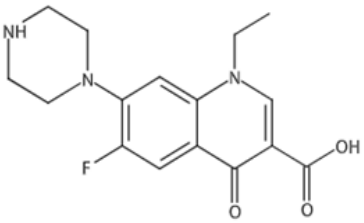
Formula	$C_8H_{10}N_4O_2$	$C_{17}H_{18}FN_3O_3$	$C_{16}H_{18}FN_3O_3$
Molecular mass (g mol^{-1})	194.19	331.34	319.33
pKa	0.520	6.43; 8.68	0.160; 8.68
Mass solubility (g L)*	58.0	0.460 - 1.60	0.350 - 1.40
Log P	0.628	1.625	1.744

* Solubility at the pH range from 7 to 9, at 25 °C; pKa = -logKa; Log P = Octanol-water partition coefficient.
Source: Adapted from SciFinder (2021).

Even at μg L^{-1} concentration level, these compounds inhibit nitrite reductase and polyphosphate kinase, reducing the removal of nitrogen and phosphorus in biological processes applied in wastewater treatment plants (WWTPs) (Yi *et al.*, 2017). Furthermore, the presence of these antibiotics and other pharmaceutical compounds in wastewater samples increases the risk of development of antibiotic resistant genes (ARG) and their transfer through the aquatic environment. Wastewaters containing pharmaceutical compounds, microbiota, plasmids, transposons, and integrons act as ARG reservoirs that can facilitate the spread of antimicrobial resistance (Osińska *et al.*, 2016).

Biochar, as an adsorbent, can be used for the removal of antibiotics and metals from aqueous solutions, with the advantages of low production costs and environmental sustainability (Liang *et al.*, 2021; Z. Li *et al.*, 2020; Tan *et al.*, 2015). Wang *et al.* (2017) used activated magnetic biochar to remove norfloxacin at concentrations in the range from 1.00 to 10.0 mg L^{-1}

Eclética Química Journal, vol. 47, n. 2, 2022, 82-96
ISSN: 1678-4618
DOI: 10.26850/1678-4618eqj.v47.2.2022.p82-96

in water solutions, achieving a removal efficiency of 97.62%. Huang *et al.* (2020) prepared biochar from rabbit feces by pyrolysis at four temperatures (400, 500, 600, and 700 °C). The biochar was then used to remove CIP at a concentration of 10 mg L^{-1} in water solutions, achieving removal efficiencies of 76.41, 96.80, 92.50, and 96.79% after 400 min.

Anastopoulos *et al.* (2020) produced oxidized biochar from pine needles at 650 °C, using boiling nitric acid. The biochar was used for to remove CAF at concentrations from 5 to 50 mg L^{-1} in water and sewage samples, reaching an adsorption capacity of 1.41 mg g^{-1} after 150 min, at pH 4.0.

Pyrolysis, torrefaction, and hydrothermal carbonization are the main processes applied for the conversion of biomass to biochar. Pyrolysis is characterized by a high heating rate to temperatures above 300 °C, which produces biochar with high surface area and pore volume. Torrefaction is performed in the temperature range between 200 and 300 °C, so the energy costs are lower and it is possible to use renewable sources, such as solar energy. The reactions during torrefaction involve carbonization, volatilization, and depolymerization of hemicellulose, cellulose, and lignin. In addition, water and lipids are converted to condensable and non-condensable gases that then generate CO_2, CO, and CH_4. Around 70% of the mass is retained as solid material and 30% is lost as condensable and non-condensable compounds (Tumuluru *et al.*, 2011). The hydrothermal carbonization is a thermochemical conversion technique, whose main characteristic is the direct application to biomass with high humidity, for the production of water-soluble organic matter and carbon-rich products at temperatures 150 - 350 °C (Liang *et al.*, 2021).

Lignocellulosic biomasses in the form of natural resources and solid residues generated by anthropic activities worldwide can be used for the production of biochar (Rangabhashiyam and Balasubramanian, 2019), being economically attractive since these raw materials are inexpensive and available in abundance.

The main sources of biochar are lignocellulosic biomasses obtained from solid residues produced in agriculture (such as sugarcane bagasse and straw), forest residues (including branches, foliage, and sawdust), and sludge from wastewater treatment plants.

Among the agricultural lignocellulosic residues, sugarcane bagasse can be highlighted as a raw material for biochar production. Brazil is the world's largest sugarcane producer, with an estimated production of more 654.5 million tons in the 2020/2021 season. São Paulo State was responsible for 354 million tons of sugarcane, accounting for 54.12% of the sugarcane processed in the country (Brazil, 2021). During sugarcane processing, bagasse is generated as a waste, corresponding to approximately 30% of the planted sugarcane (Jayaraman *et al.*, 2018). Currently, most of this material is burned to produce energy in the boilers in the sugar and ethanol plants.

Sugarcane bagasse is composed, on average, of 40-45% cellulose, 25 - 30% hemicellulose, and 20 - 25% lignin. It has a heterogeneous surface that presents phenolic groups, carboxylic acids, and hydroxyls (Ramos *et al.*, 2016). The use of sugarcane bagasse as raw material for biochar is attractive because it is abundant and inexpensive, with an estimated price of around US$ 20.00 per ton.

The aim of this work was to evaluate the physicochemical properties of sugarcane bagasse biochars obtained using a torrefaction process at four different temperatures (260, 270, 280, and 290 °C). The biochars were tested as adsorbents for the removal of CAF, CIP, and NOR present in lab-made sewage samples. This study purpose to use this inexpensive and abundant adsorbent material, without need for chemical or physical activation, for the specific removal of these emerging contaminants found at µg L^{-1} concentration level.

2. Materials and methods

2.1 Chemicals and reagents

The pharmaceutical compounds CAF, CIP, and NOR were acquired from Sigma-Aldrich (Saint Louis, MO, USA). The solvents (HPLC grade) methanol, acetonitrile, and 88% formic acid were purchased from J.T. Baker (Phillipsburg, NJ, USA).

The lab-made sewage composition was as follows: cellulose (47.0 mg L^{-1}), sucrose (98.0 mg L^{-1}), starch (149 mg L^{-1}), $NaHCO_3$ (370 mg L^{-1}), meat extract (262 mg L^{-1}), NaCl (250 mg L^{-1}), $CaCl_2$ (7.00 mg L^{-1}), $MgCl_2$ (4.50 mg L^{-1}), LAS (surfactant, 1.00 mg L^{-1}), K_2HPO_4, and soybean oil (79 mg L^{-1}). These compounds were dissolved in tap water and resulted in a chemical oxygen demand (COD) of 550 mg O_2 L^{-1} and a pH value of 8.0.

2.2 Biochar preparation

The Santa Cruz sugar and ethanol plant (São Martinho Group) located in Américo Brasiliense (São Paulo State, Brazil; 21°45'09.5"S, 48°04'51.3"W) donated the sugarcane bagasse (from sugarcane variety

Eclética Química Journal, vol. 47, n. 2, 2022, 82-96
ISSN: 1678-4618
DOI: 10.26850/1678-4618eqj.v47.2.2022.p82-96

RB855156). The bagasse was triturated in an industrial blender, sieved through a 2 mm mesh, and transformed into pellets using a hydraulic press machine at 7 atm. As a way to standardize the size of the pellets produced, a stainless-steel mold was used, in order to obtain pellets with a diameter of 12 mm each.

The samples were torrefied in atmospheric conditions (altitude of 664 meters, atmospheric pressure 1012 hPa). Four different torrefaction temperatures were tested, with evaluation of the resulting biochars in terms of their physicochemical characteristics and mechanical resistance in an aqueous medium. The temperatures used were 260, 270, 280, and 290 °C, producing biochars denoted BG260C, BG270C, BG280C, and BG290C, respectively. The pelleted bagasse samples were placed in porcelain crucibles and torrefied in a muffle furnace (Model 7000, EDG Solutions, São Carlos, SP, Brazil). The oven program started at 40 °C, with a ramp rate of 10 °C min^{-1} and a residence time of 1 h after reaching the desired temperature (this time was necessary for the pellets not to break easily). After the process, the crucibles were removed and placed in a desiccator. The biochar pellets were washed in water for 2 h, under stirring at 125 rpm, in a shaker-incubator (Model MA830, Marconi, Piracicaba, SP, Brazil) for the removal of ash and impurities derived from the torrefaction process, followed by drying for 24 h at 120 °C. Figure 1 shows the workflow for production of the biochar pellets by torrefaction.

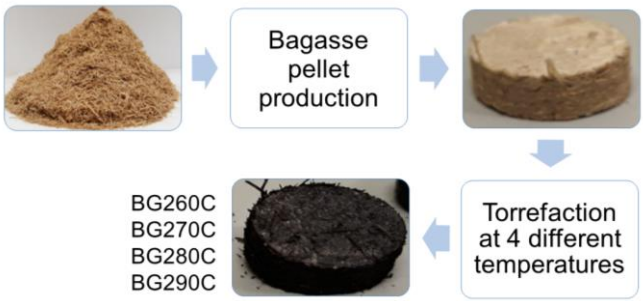

Figure 1. Sugarcane bagasse biochar torrefaction and pellet production processes.

2.3 Characterization of the materials

2.3.1 Thermogravimetry and proximate analysis

Thermogravimetric analysis (TGA) was performed using an SDT-2960 Simultaneous TGA/DTA (differential thermal analysis) Thermal Analyzer (TA Instruments, New Castle, DE, USA). For the characterization by TGA/DTG (derivative thermogravimetry), the thermal analyzer software was programmed for two evaluation methods: thermal stability and proximate analysis.

For the thermal stability analysis, the biochar sample was macerated and approximately 8 mg were placed in an alumina crucible for weighing using the thermobalance. The sample was heated under an atmosphere of synthetic air at a flow rate of 100 mL min^{-1}, with the temperature increased from 25 to 600 °C at a rate of 10 °C min^{-1}.

For the proximate analysis, about 9 mg of the macerated biochar were weighed out and placed in an alumina crucible, according to the method described previously (Torquato *et al.*, 2017).

2.3.2 Scanning electron microscope

Topographic contrast micrographs were obtained using a scanning electron microscope (SEM) (Model JSM7500F, JEOL, Kyoto, Japan). The SEM images were acquired at magnifications of 100x and 7000x.

2.3.3 Fourier transform infrared absorption spectroscopy

Fourier transform infrared absorption spectroscopy (FTIR) spectra were acquired in the range from 4000 to 400 cm^{-1}, using a spectrophotometer (Vertex 70, Bruker, Billerica, MA, USA) equipped with an attenuated total reflectance (ATR) accessory.

2.3.4 Elemental analysis

Elemental analysis was performed using a CNHS/O 2400 Series II Elemental Analyzer (Perkin Elmer, Waltham, MA, USA) to determine the sample composition in terms of carbon (C), hydrogen (H), nitrogen (N), sulfur (S), and oxygen (O).

2.3.5 Surface area analysis

The biochar surface area and porosity were measured using the nitrogen adsorption and desorption method. The isotherms were recorded using an ASAP 2000 instrument (Micromeritics, Narcross, GA, USA) operated with ASAP 2010 v. 3.01 software.

2.3.6 Point of zero charge and pH

The pH was measured using a pH meter (Model PG1800, Gehaka, São Paulo, SP, Brazil). The point of zero charge (pH_{PZC}) determination was performed using

Eclética Química Journal, vol. 47, n. 2, 2022, 82-96
ISSN: 1678-4618
DOI: 10.26850/1678-4618eqj.v47.2.2022.p82-96

the method proposed by Regalbuto and Robles (2004), employing 30 mL of deionized water with 30 mg of crushed biochar. The pH was adjusted with solutions of hydrochloric acid (HCl) and sodium hydroxide (NaOH), both at 0.100 mol L^{-1}, in order to obtain pH values of 2, 3, 4, 5, 6, 7, 8, 9, 10, 11, and 12. After 24 h, the pH was measured again.

The pH analysis was conducted according to the method proposed by Ahmedna *et al.* (1997). The experiments were performed for each biochar sample, which was crushed and added to deionized water (1% w/w). The solution was heated to 90 °C and kept under stirring for 20 min. After this period, the samples were cooled to room temperature and the pH was measured again.

2.4 Adsorption experiments

2.4.1 Selection of torrefaction temperature

The BG260C, BG270C, BG280C, and BG290C biochar pellets were evaluated for the adsorption of CAF at a concentration of 5.00 µg L^{-1} in ultrapure water. The assays were performed during 24 h, at a controlled temperature of 25 °C, with stirring at 100 rpm, using a shaker-incubator (Model MA830, Marconi, Piracicaba, SP, Brazil). These tests were carried out together with a control experiment using 5.00 µg L^{-1} CAF solution without the adsorbent material. Aliquots of 500 µL were withdrawn from the solution at different times (0, 0.25, 0.5, 1, 2.5, 5, 10, and 24 h), in order to evaluate the adsorption kinetics.

2.4.2 Kinetics of adsorption of the pharmaceutical compounds onto the biochar in lab-made sewage

Lab-made sewage produced in the laboratory was used, since it enabled simulation of the composition of domestic sewage, in the absence of any preexisting pharmaceutical compounds. The adsorption of CAF, CIP, and NOR was evaluated using the biochar obtained using the best torrefaction temperature. The batch adsorption tests were performed individually for each pharmaceutical compound, in order to avoid possible synergistic interactions and interference in this experiment. For this adsorption kinetics, in 100 mL polypropylene flasks, approximately 6.0 g (equivalent 30 mL) of biochar and 60 mL of lab-made sewage were added.

The lab-made sewage was spiked with each compound, using concentrations of 5.00 µg L^{-1} for CAF and 10.0 µg L^{-1} for CIP and NOR. The test was carried out during 24 h, at a controlled temperature of 25 °C and with stirring at 100 rpm. A control experiment with each individual pharmaceutical compound was performed using only the lab-made sewage, without the adsorbent material.

Aliquots of 500 µL were withdrawn from the solution at 10 different times (0, 0.5, 1, 2, 3, 4, 6, 8, 10, and 24 h), for determination of the adsorption kinetics. The samples were filtered through 0.22 µm nylon membranes and analyzed by LC-MS/MS, according to the method developed by Marasco Júnior *et al.* (2021). In this developed method the limits of detection and quantification were, respectively, for CAF 0.001 and 0.5 µg L^{-1}; CIP 0.5 and 3 µg L^{-1} and for NOR 1 and 3 µg L^{-1}.

3. Results and Discussion

3.1 Thermogravimetric analysis

3.1.1 Thermogravimetry / derivative thermogravimetry

Figure 2 shows the TGA/DTG curves for the in natura bagasse (BG) and the biochars BG260C, BG270C, BG280C, and BG290C, indicating three well-defined thermal events. The first event did not involve decomposition, but was due to the elimination of moisture present in the samples. The curves showed that with increase of the torrefaction temperature, the biochar presented a lower content of hydrophilic components and consequently absorbed a smaller amount of moisture.

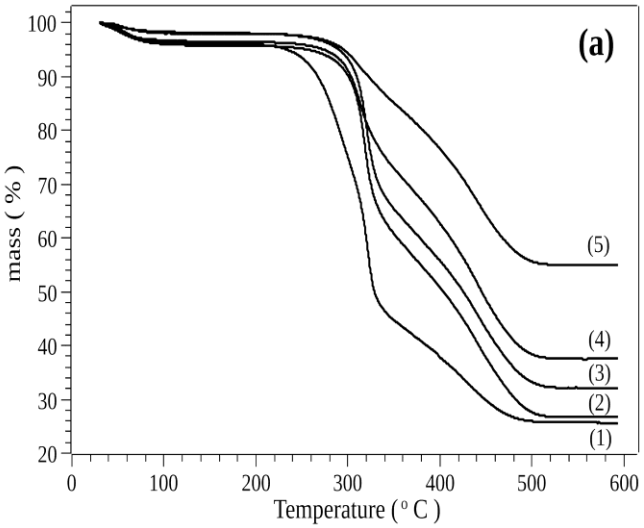

Eclética Química Journal, vol. 47, n. 2, 2022, 82-96
ISSN: 1678-4618
DOI: 10.26850/1678-4618eqj.v47.2.2022.p82-96

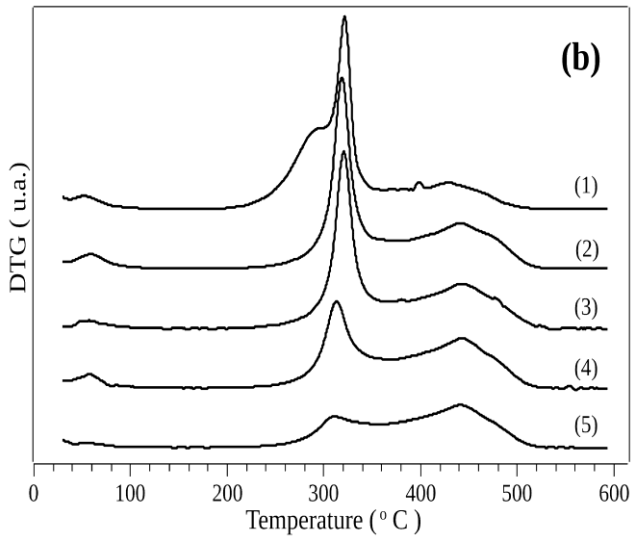

Figure 2. TGA **(a)** and DTG **(b)** curves obtained for the in natura bagasse (1), BG260C (2), BG270C (3), BG280C (4), and BG290C (5).

The second thermal event was associated with the decomposition of hemicellulose and cellulose. The TGA/DTG curves indicated that the in natura bagasse was less stable, with the thermal decomposition temperature being shifted to the left and the presence of two superimposed peaks attributed to hemicellulose and cellulose. The BG290C sample showed greater stability, with the temperature for initiation of decomposition shifted to the right, due to previous elimination of volatile material during the torrefaction.

The third decomposition step could be attributed to lignin, with thermal decomposition between 350 and 530 °C. The TGA curves showed that higher thermal stability was correlated with higher biochar torrefaction temperature.

This increase of stability was related to the amount of residues and metal oxides present in the sugarcane bagasse pellets.

Table 2 shows the mass losses in each temperature range, the mass loss variation in the stages, the residue produced, and the total mass loss for each sample. The moisture losses ranged from 1 to 4% (Fig. 2, Tab. 3), with these low values suggesting that partial degradation of hemicellulose, cellulose, and lignin occurred during pellet torrefaction.

Table 2. Mass loss event temperature ranges (ΔT), mass losses (Δm), sample ash contents, and total mass losses for the in natura bagasse and the biochars.

Sample	ΔT (°C)	Δm (%)	Ash (%, at 591.6 °C)	Total mass loss (%)
Raw BG	1st) 30.3 – 105	3.68	25.6	74.4
	2nd) 195 – 376	54.7		
	3rd) 376 – 518	15.5		
BG260C	1st) 21.6 – 113	4.06	26.6	73.4
	2nd) 186 – 360	39.4		
	3rd) 360 – 517	29.6		
BG270C	1st) 22.4 – 90.0	1.80	32.2	67.8
	2nd) 204 – 356	37.2		
	3rd) 356 – 516	28.6		
BG280C	1st) 26.6 – 94.4	3.24	37.5	62.5
	2nd) 208 – 362	27.0		
	3rd) 362 – 541	31.8		
BG290C	1st) 41.0 – 106	1.24	54.9	45.1
	2nd) 163 – 347	12.9		
	3rd) 361 – 529	27.9		

Table 3. Average compositions of the raw bagasse and the biochars, in terms of moisture, volatile materials, fixed carbon, and ash.

Sample	Composition (%)			
	Moisture	Volatile materials	Fixed carbon	Ash
Raw BG	3.96	51.2	7.67	36.9
BG260C	3.25	48.7	20.3	27.6
BG270C	3.82	31.5	27.8	36.9
BG280C	2.57	27.0	24.5	45.8
BG290C	2.58	40.1	28.2	29.1

Eclética Química Journal, vol. 47, n. 2, 2022, 82-96
ISSN: 1678-4618
DOI: 10.26850/1678-4618eqj.v47.2.2022.p82-96

In the second step, it could be seen that increase of the torrefaction temperature led to a decrease of the peak related to the mass loss attributed to hemicellulose and volatile compounds, which was greatest for the biochars produced at 280 and 290 °C, since these higher temperatures caused substantial losses of these components.

In the third step, the cellulose and lignin degradation peaks were less intense, compared to the peaks of the second stage. For BG260C and BG270C, the mass loss was higher in the second stage than in the third stage, while the opposite was observed for samples BG280C and BG290C. This suggested that lignin and cellulose were the main components present in BG280C and BG290C. In addition, increase of the torrefaction temperature led to an increase of the ash content, relative to the other fractions (Tab. 2).

Increase of the torrefaction temperature was directly related greater decomposition of the organic content. At high temperatures, the losses affect the mechanical properties, porosity, density, and thermal stability of the material.

3.1.2 Proximate analysis

In the torrefaction temperature range (200-300 °C), increase of the mass loss was directly related to the temperature increase, mainly due to the decomposition of hemicellulose, as shown in Fig. 2 and Tab. 2. When pyrolysis is performed at temperatures above 300 °C, the main mass loss and consequent generation of volatile materials are associated with the decomposition of cellulose and lignin (Dias *et al.*, 2018).

The amounts of water found in the biochars and the in natura bagasse corresponded to the combination of surface humidity and the moisture present within the composition of the material. The moisture contents presented by the biochars and the bagasse did not exceed 4% (Tab. 3).

As expected, the in natura bagasse presented the highest mass loss due to volatile materials (51.2%), since the previously torrefied samples had already partially lost these compounds.

3.2 Scanning electron microscopic analyses

The micrographs of the biochars (Fig. 3) obtained at magnifications of 100x and 7000x showed that increase of the torrefaction temperature caused an increase of the amount of carbonized biomass, with small fragments evident. It could also be seen that the biochar surface was not regular, due to partial removal of the lignocellulosic biomass during the torrefaction process, leaving the biochar with a porous and rough surface. This indicated the suitability of the material for use as an adsorbent, since a high surface area enables efficient interaction with different types of chemical compounds.

The porous structure demonstrated that the thermal conversion process removed the outer fibers, consequently increasing the surface area, which made the cellulose accessible for thermal degradation (Morais *et al.*, 2017). The formation of irregular particles could have been related to the fusion and solidification of oxides formed between silicon, metal elements, and oxygen during combustion. The silicon content in biochar is a favorable aspect for its use as an adsorbent material, since a high silicon content promotes the ionic exchange of metallic species (Rodríguez-Díaz *et al.*, 2015).

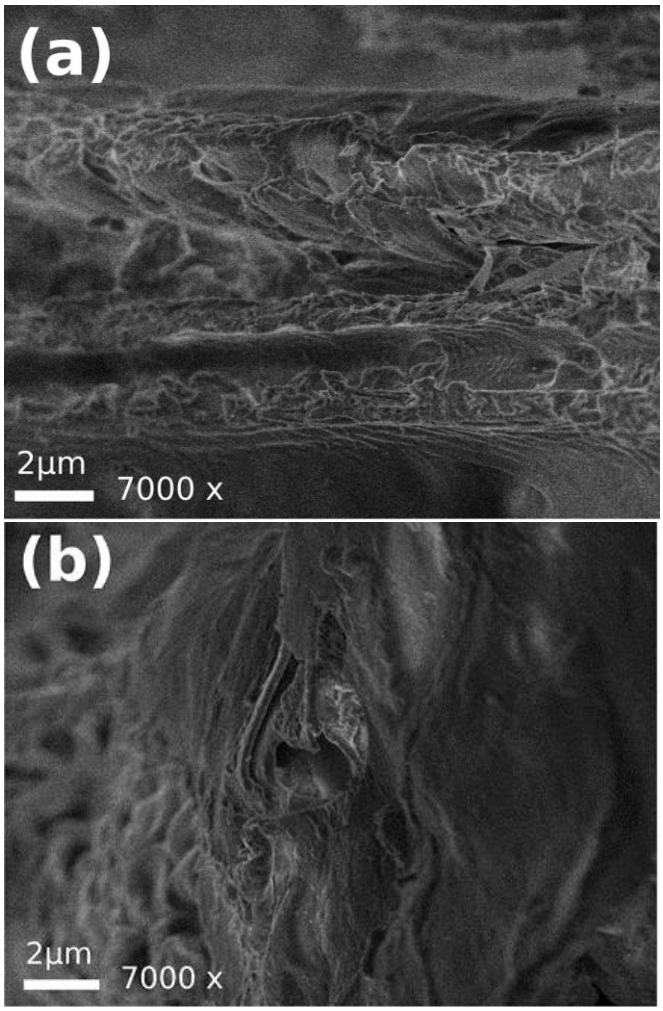

Eclética Química Journal, vol. 47, n. 2, 2022, 82-96
ISSN: 1678-4618
DOI: 10.26850/1678-4618eqj.v47.2.2022.p82-96

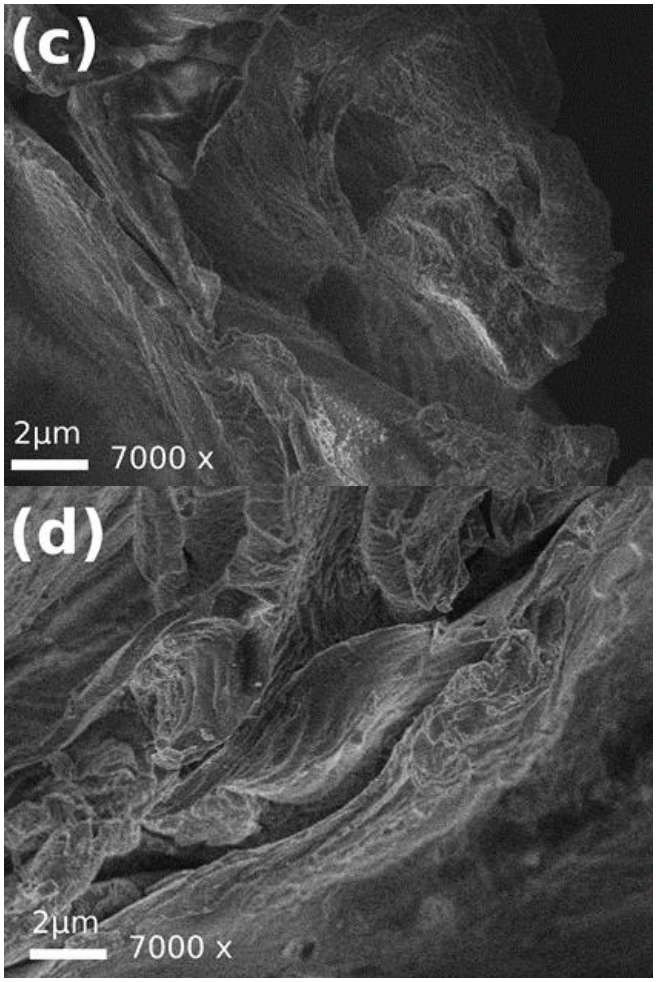

Figure 3. Scanning electron microscopic micrographs of the biochars at magnification of 7000x: BG260C **(a)**, BG270C **(b)**, BG280C **(c)**, and BG290C **(d)**.

3.3 Fourier transform infrared analysis of the biochars

Figure 4 shows the FTIR spectra obtained in the range from 4000 to 400 cm^{-1}.

Bands in the region between 3700 and 3100 cm^{-1} could be attributed to O–H bond stretching, due to the presence of alcoholic, phenolic, and hydroxyl groups in the lignocellulosic biomass. Bands in the range 3000–2700 cm^{-1} corresponded to asymmetric and symmetric stretching of methyl and methylene groups, respectively (Becker *et al.*, 2013; Granados *et al.*, 2017). Bands in the region between 1800 and 1650cm^{-1} were due to carbonyl group stretching, indicating the presence of conjugated and unconjugated C=O of carboxylic acids from hemicellulose and from cellulose after oxidation.

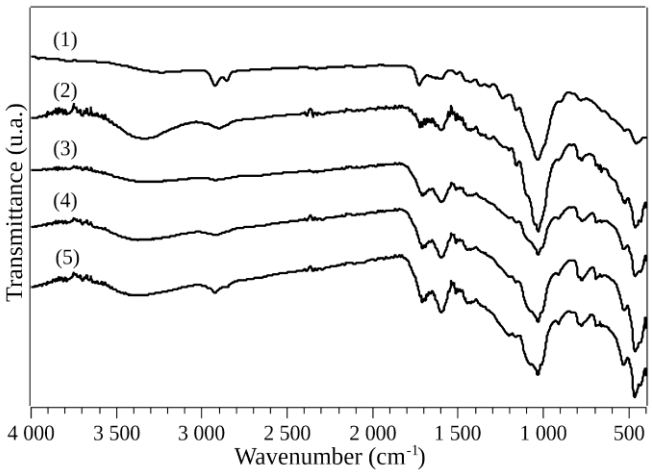

Figure 4. Infrared spectra of the in natura bagasse (1), BG260C (2), BG270C (3), BG280C (4), and BG290C (5) in the 4000–400 cm^{-1} region.

The torrefaction process led to decreased intensity of this peak, reflecting a decrease of carboxylic acid groups, leading to the formation of new products, as shown by signals at around 1700 cm^{-1}.

Signals in the range 1600–1500 cm^{-1} could be attributed to vibrations of C=C in the lignin aromatic skeleton, which increased as the torrefaction temperature increased. Bands between 1500 and 1350 cm^{-1} corresponded to deflections and deformations of C–H bonds of amorphous lignin and cellulose polysaccharides. Bands in the range 1300–1150 cm^{-1} were due to stretching vibrations of C–O of the lignin guaiacyl aromatic rings and antisymmetric stretching of the C–OH and C–O–C bonds of cellulose and hemicellulose. The intensity of the bands in this region tended to decrease with increase of the torrefaction temperature. Bands in the range 1050–1000 cm^{-1} corresponded to C–O, C=C, and C–C vibrations of cellulose, hemicellulose, and lignin. A small band at around 900 cm^{-1} could be attributed to the beta-glycosidic bonds in cellulose and hemicellulose, while bands in the range 800–600 cm^{-1} were due to the vibrations of O–H connections (Granados *et al.*, 2017; Ibrahim *et al.*, 2013; Mubarik *et al.*, 2015; Rodríguez-Díaz *et al.*, 2015). The FTIR data is presented in Tab. 4.

Eclética Química Journal, vol. 47, n. 2, 2022, 82-96
ISSN: 1678-4618
DOI: 10.26850/1678-4618eqj.v47.2.2022.p82-96

Table 4. Possible functional groups and compounds found in the samples by FTIR.

Wavenumber (cm^{-1})	Type of vibration	Chemical functionalities and/or possible components	References
3700-3100	O–H	Alcoholic, phenolic, and hydroxyl groups	Granados *et al.* (2017); Mubarik *et al.* (2015); Rodríguez-Díaz *et al.* (2015)
3000-2700	C–H	Methyl and methylene	Granados *et al.* (2017)
1800-1650	C=O	Carboxylic acid	Granados *et al.* (2017); Mubarik *et al.* (2015); Rodríguez-Díaz *et al.* (2015)
1600-1500	C=C	Aromatics	Mubarik *et al.* (2015)
1500-1350	C–H	Amorphous polysaccharides	Granados *et al.* (2017)
1300-1150	C–O, C–OH, C–O–C	Aromatics, lignin, cellulose, and hemicellulose	Granados *et al.* (2017); Mubarik *et al.* (2015)
1050-1000	C–O, C=C, C–C–O	Cellulose, hemicellulose, and lignin	Granados *et al.* (2017)
900	β-glycoside	Hemicellulose and cellulose	Granados *et al.* (2017)
800-600	O–H	Alcoholic, phenolic, and hydroxyl groups	Granados *et al.* (2017)

3.4 Biochar elemental composition

The elemental compositions of the biochars are shown in Tab. 5. As expected, there was an increase of the carbon content as the temperature increased, while the hydrogen, oxygen, and sulfur contents decreased. Higher nitrogen contents were found for the biochars produced at 280 and 290 °C, compared to those produced at 260 and 270 °C.

In general, as the torrefaction temperature and residence time increase, there are increases of the amount of carbon and decreases of the amounts of hydrogen and oxygen. Therefore, the values of the H/C and O/C atomic ratios tend to decrease with increase of the torrefaction temperature (Tumuluru *et al.*, 2011).

Slight decreases of the H/C and O/C ratios values were observed as the torrefaction temperature increased, which could be explained by the loss of hydroxyl and carboxylic functional groups, respectively (Rangabhashiyam and Balasubramanian, 2019). Lower O/C values were observed according to increase of the temperature, indicating a more aromatic biochar and a less hydrophilic structure, due to dehydration reactions and the higher degree of carbonization.

Table 5. Elemental compositions and atomic ratios of the biochars.

Elements and ratios	Composition (%)			
	BG260C	BG270C	BG280C	BG290C
Carbon (C)	49.5	50.7	52.2	54.1
Hydrogen (H)	4.19	3.91	2.54	2.33
Nitrogen (N)	0.15	0.14	0.35	0.27
Sulfur (S)	1.02	0.96	0.64	0.66
Oxygen (O)	30.9	30.0	29.3	20.4
Ratio H/C	0.08	0.08	0.05	0.04
Ratio O/C	0.62	0.59	0.56	0.38
Ratio (O+N)/C	0.63	0.60	0.57	0.38

The low H/C values indicated that the biomass was carbonized, suggesting an increase of aromaticity as the torrefaction temperature increased. However, the biochar produced was not totally hydrophobic and aromatic, since the FTIR spectra showed the presence of bands corresponding to hydrophilic groups. This was also observed by Al-Wabel *et al.* (2013), who found that the H/C ratio decreased using temperatures in the range from 200 to 800 °C. Hafshejani *et al.* (2016) compared a sample of in natura sugarcane bagasse with bagasse pyrolyzed at 300 °C and observed an increase from 0.3 to 4.1%.

Eclética Química Journal, vol. 47, n. 2, 2022, 82-96
ISSN: 1678-4618
DOI: 10.26850/1678-4618eqj.v47.2.2022.p82-96

3.5 Surface area

The results obtained for the BET surface area, pore total volume, and pore size of the biochars are presented in Tab. 6.

The use of torrefaction temperatures from 260 to 290 °C, with heating rates of 10 °C min^{-1} and short residence times (1 h), resulted in BET surface areas ranging from 1.83 to 3.24 m^2 g^{-1}. The small variation in the torrefaction temperature did not significantly alter the surface areas. The BG280C sample presented the highest values for the surface area and the pore volume. This biochar also showed the highest release of volatile materials, as shown by the proximate analysis.

Sun *et al.* (2018) pyrolyzed sugarcane bagasse at temperatures ranging from 300 to 600 °C, with a residence time of 2 h and heating rate of 5 °C min^{-1}, obtaining a surface area and total pore volume of 1.05 m^2 g^{-1} and 0.68 cm^3 g^{-1}, respectively, for the sample produced at 300 °C. In other work, peanut shells were used for biochar production, with specific surface areas of 1.83 and 7.11 m^2 g^{-1} obtained at temperatures of 200 and 300 °C, respectively (J. Chen *et al.*, 2017; W.-H. Chen *et al.*, 2017).

Table 6. BET surface areas, pore total volumes, and pore sizes of the biochars.

Sample	BET surface area (m^2 g^{-1})	Pore total volume (cm^3 g^{-1})	Pore size (Å)
BG260C	1.83	5.1 x 10^{-3}	112
BG270C	2.08	5.5 x 10^{-3}	126
BG280C	3.24	6.2 x 10^{-3}	108
BG290C	2.04	6.1 x 10^{-3}	121

3.6 Determination of pH and pH_{PZC}

The values obtained for the point of zero charge and pH are provided in Tab. 7.

Table 7. pH_{PZC} and pH values of the biochars.

Sample	pH_{PZC}	pH
BG260C	4.61 ± 0.52	4.38 ± 0.08
BG270C	5.01 ± 0.73	4.43 ± 0.08
BG280C	5.64 ± 0.06	4.60 ± 0.03
BG290C	5.53 ± 0.56	4.58 ± 0.09

The pH_{PZC} ranged from 4.61 to 5.53, while the pH ranged from 4.38 to 4.60. The solution pH was lower than the pH_{PZC}, indicating that the sugarcane bagasse biochar presented a positive surface charge, related to an excess of H+ ions capable of adsorbing anionic species (Binh and Nguyen, 2020). These results were in agreement with the findings of Hafshejani *et al.* (2016), which obtained a pH_{PZC} of 5.35 for torrefied biochar produced from modified sugarcane bagasse.

As the torrefaction temperature increased, there was a small increase of the pH, which could be explained by the separation of alkaline salts from organic materials (Al-Wabel *et al.*, 2013; Tag *et al.*, 2016). The alkalinity and carbonate content of biochars tend to increase as the temperature increases, while the contribution of organic anions to biochar alkalinity decreases (Yuan *et al.*, 2011).

3.7 Adsorption kinetics

3.7.1 Selection of torrefaction temperature

The choice to prepare pellets by torrefaction was based on lower energy costs, in addition to the possibility of using renewable sources, such as solar energy (Quéno *et al.*, 2019). In order to identify the best biochar torrefaction temperature, preliminary experiments were performed using 5.00 µg L^{-1} CAF in aqueous solution. The CAF removal efficiencies are shown in Tab. 8. CAF was selected since it is an important emerging contaminant, considered as a biomarker of anthropogenic contamination of wastewater and surface waters (Buerge *et al.*, 2003).

The biochar samples showed similar behaviors, with removal efficiencies higher than 88% and attainment of equilibrium in approximately 10 h, with the exception of BG270C, for which equilibrium was reached after 24 h. After 24 h of the experiment, the BG260C pellets underwent disintegration, with the solution presenting a yellow color (data not shown). The BG270C and BG290C samples showed partial disintegration of some biochar pellets, but no color change of the solution. The BG280C sample presented the best stability in the aqueous medium, without disintegration or solution color change. Therefore, the BG280C sample was selected for use as an adsorbent, since it presented the best stability in solution and showed a CAF adsorption efficiency of 92.8% after 10 h, in comparison to the control.

Table 8. Removal efficiencies obtained for CAF at 5.00 µg L^{-1} in aqueous solution, using the BG260C, BG270C, BG280C, and BG290C biochars.

CAF removal efficiency (%)				
t (h)	Biochar sample			
	BG260C	BG270C	BG280C	BG290C
10	89.61	92.50	92.84	90.29
24	88.25	93.53	91.82	89.95

Eclética Química Journal, vol. 47, n. 2, 2022, 82-96
ISSN: 1678-4618
DOI: 10.26850/1678-4618eqj.v47.2.2022.p82-96

3.7.2 Adsorption of the pharmaceutical compounds on biochar pellets in lab-made sewage

The BG280C biochar was chosen as the adsorbent material. Contact time experiments were carried out for CAF, CIP, and NOR in three separate assays employing the lab-made sewage pH 8.0 (COD of 550 mg O_2 L^{-1}) simulating the composition of domestic sewage. Figure 5 presents the removal efficiencies obtained for these three compounds.

In this study the main objective was to remove the CAF, CIP and NOR using the biochar in complex samples, such as lab-made sewage which mimics the soluble components of domestic sewage and present pH equal to 8. Therefore, the pH tests were not carried out to investigate possible effects of this parameter in the removal process. All batch studies were performed at pH equal to 8.

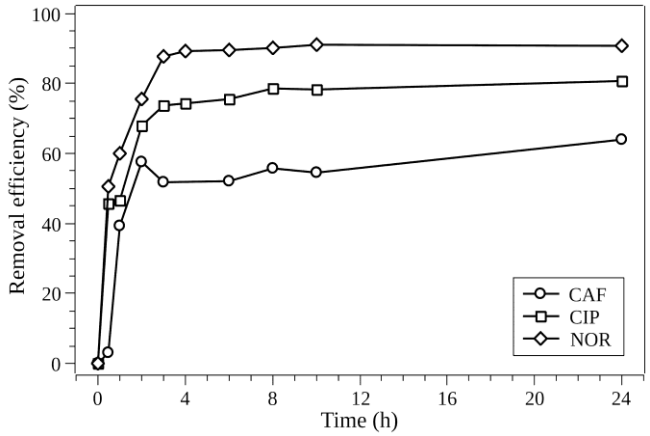

Figure 5. Removal efficiencies obtained for CAF at 5.00 µg L^{-1}, CIP at 10.0 µg L^{-1}, and NOR at 10.0 µg L^{-1}, using the BG280C biochar in lab-made sewage.

NOR and CIP presented similar adsorption behaviors, with removal efficiencies of 91.0 and 81.0%, respectively and attainment of equilibrium after around 4 and 8 h, respectively. This removal could be attributed to the positive charges present on the surface of the biochar pellets, which attracted the negative parts of the CIP and NOR molecules in the lab-made sewage with pH 8.0. These molecules exist in zwitterionic forms in solutions with pH from 6.0 to 8.8 (Osonwa *et al.*, 2017; Sun *et al.*, 2002).

In the case of CAF, there was a decrease of the adsorption between 3 and 4 h, with equilibrium being reached after 6 h. A total of 58.0% of CAF was removed from the lab-made sewage, which was lower than the value of 92.8% obtained in the earlier experiment using the compound in ultrapure water.

The observed difference in the CAF removal efficiency could be explained by the compositional complexity of the lab-made sewage, compared to ultrapure water. In particular, the presence of chloride ions and soybean oil can interfere in the adsorption efficiency.

As mentioned previously, the π-π interactions of the biochar with the aromatic rings of the compounds could have contributed to the adsorption. As indicated by the results of the FTIR and elemental composition analyses, the presence on BG280C of groups containing electronegative elements such as oxygen and nitrogen provided abundant sites for adsorption (Tran *et al.*, 2017).

The keyhole pore filling mechanism could have contributed to the adsorption of the compounds. CIP presents dimensions of 13.5 × 3 × 7.4 Å, so it (as well as CAF) could be adsorbed by this mechanism, since the dimensions of the molecules were smaller than those of the biochar pores (Ma *et al.*, 2017). Figure 6 shows the removal efficiencies obtained using the BG280C biochar in the lab-made sewage.

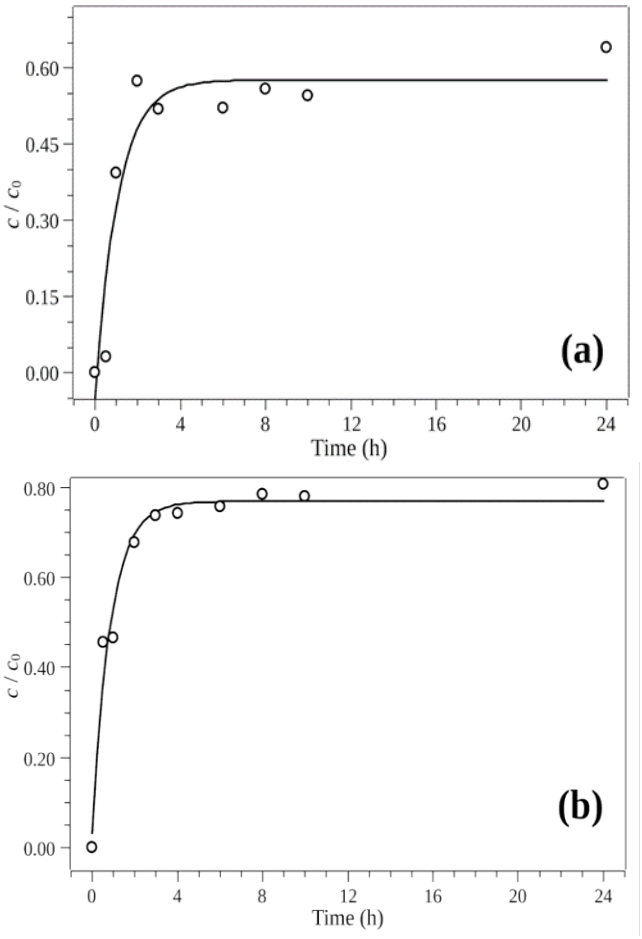

Eclética Química Journal, vol. 47, n. 2, 2022, 82-96
ISSN: 1678-4618
DOI: 10.26850/1678-4618eqj.v47.2.2022.p82-96

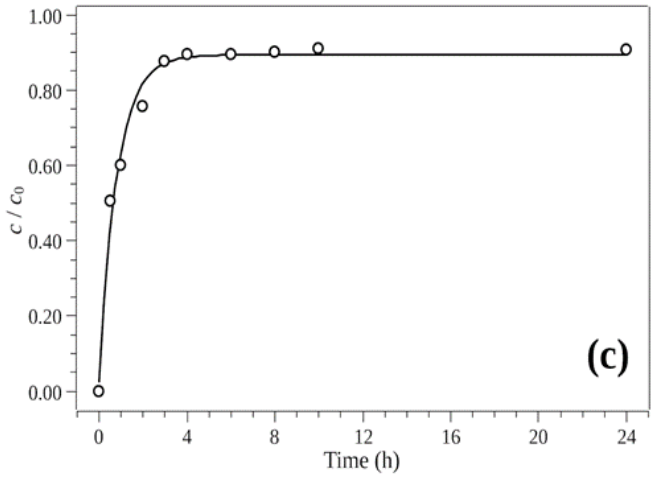

Figure 6. Removal efficiencies obtained for CAF at 5.00 µg L^{-1} **(a)**, CIP at 10.0 µg L^{-1} **(b)**, and NOR at 10.0 µg L^{-1} **(c)**, using the BG280C biochar in lab-made sewage.

The compounds NOR, CAF, and CIP reached equilibrium after periods of 4, 6, and 8 h, respectively. As shown from the pH/pH_{PCZ} results, the sugarcane bagasse biochar samples had positive charges on their surfaces, due to the excess of H+ ions. Therefore, the adsorption of a cationic species such as CAF occurred due to other interaction mechanisms.

The presence of functional groups rich in oxygen on the adsorbent surface can contribute to the adsorption of contaminants. In addition, π–π interactions of electron donors and acceptors are important in removal by adsorption. The FTIR and elemental analyses of the biochars demonstrated the presence of carboxylic acids and nitrogenous groups. Therefore, π–π interactions could have contributed to the adsorption of CAF on the torrefied sugarcane bagasse. As reported previously, carboxylic acids and carbonyls tend to be electron acceptors in the formation of π–π interactions with aromatic molecules, contributing to CAF adsorption (Ahmed *et al.*, 2018; Keiluweit and Kleber, 2009).

The adsorption of CAF could also have been favored by the biochar pore size, which varied from 108 to 126 Å, since the caffeine molecule has dimensions of 7.8 × 6.1 × 2.1 Å, enabling its penetration into the biochar pores (Pendolino, 2014). Correa-Navarro *et al.* (2020) produced a biochar from fique bagasse, using pyrolysis at 850 °C and a residence time of 3 h, which was used for the removal of caffeine and diclofenac.

4. Conclusions

In this paper, torrefaction was used as a carbonization strategy, as a way to prepare sugarcane bagasse biochar which presented a high performance in the adsorption of pharmaceutical compounds. Characterization of sugarcane bagasse biochar samples using thermogravimetric and proximate analyses demonstrated the presence of lignin and cellulose as the main constituents after the thermochemical conversion. The biochars could be considered mesoporous adsorbents, with irregular and positively charged surfaces. The FTIR spectra showed the presence of hydrophilic and hydrophobic groups. Samples of the BG260C, BG270C, BG280C, and BG290C biochars were evaluated for the adsorption of CAF in aqueous media. The BG280C material presented the best adsorption efficiency (up to 93%) and stability in the aqueous media. High adsorption efficiency was achieved even at low concentrations of contaminants (at the µg L^{-1} concentration level) in a complex matrix such as lab-made sewage, where adsorptions of 91, 81, and 58% were achieved for NOR, CIP, and CAF, respectively. In addition, the low cost per ton (around US$ 20.00) of the raw material provides to sugarcane bagasse biochar a promising adsorbent and economic alternative to be used as technology to mitigate the presence of emerging contaminants in wastewater treatment plants and water supply units.

Authors' contribution

Conceptualization: Fonsêca, M. C.; Lima Gomes, P. C. F.; Pires, L. O.; Ribeiro, C. A.
Data curation: Fonsêca, M. C.; Lima Gomes, P. C. F.
Formal Analysis: Fonsêca, M. C.; Marasco Júnior, C. A.; Lima Gomes, P. C. F.
Funding acquisition: Lima Gomes, P. C. F.
Investigation: Fonsêca, M. C.; Lima Gomes, P. C. F.; Dias, D. S.
Methodology: Lima Gomes, P. C. F.; Pires, L. O.; Ribeiro, C. A.
Project administration: Lima Gomes, P. C. F.
Resources: Lima Gomes, P. C. F.
Software: Fonsêca, M. C.; Lima Gomes, P. C. F.; Pires, L. O.
Supervision: Lima Gomes, P. C. F.; Pires, L. O.
Validation: da Silva, J. P.; Marasco Júnior, C. A.
Visualization: Lima Gomes, P. C. F.; Pires, L. O.; Lamarca, R. S.

Eclética Química Journal, vol. 47, n. 2, 2022, 82-96
ISSN: 1678-4618
DOI: 10.26850/1678-4618eqj.v47.2.2022.p82-96

Writing – original draft: Fonsêca, M. C.; Lima Gomes, P. C. F.; Pires, L. O; Lamarca, R. S.
Writing – review & editing: Fonsêca, M. C.; Lima Gomes, P. C. F.; Pires, L. O; Lamarca, R. S.; Ribeiro, C. A.

Data availability statement

The data are available in the UNESP repository. The data that support the findings of this study are available from the corresponding author, Paulo C. F. Lima Gomes, upon reasonable request.

Funding

Fundação de Amparo à Pesquisa do Estado de São Paulo (FAPESP). Grant No: 2016/03369-3; 2018/22393-8; 2018/11700-7.

INCT-DATREM. Grant No: 2014/50945-4.

Conselho Nacional de Desenvolvimento Científico e Tecnológico (CNPq). Grant No: 465571/2014-0.

Coordenação de Aperfeiçoamento de Pessoal de Nível Superior (CAPES). Grant No: 88887136426/2017/00.

Acknowledgments

The authors are grateful for the support provided by Institute of Chemistry (Araraquara, São Paulo State University).

References

Ahmed, M. B.; Zhou, J. L.; Ngo, H. H.; Johir, Md. A. H.; Sun, L.; Asadullah, M., Belhaj, D. Sorption of hydrophobic organic contaminants on functionalized biochar: Protagonist role of π-π electron-donor-acceptor interactions and hydrogen bonds. *J. Hazard. Mater.* **2018**, *360*, 270–278. https://doi.org/10.1016/j.jhazmat.2018.08.005

Ahmedna, M.; Johns, M. M.; Clarke, S. J.; Marshall, W. E.; Rao, R. M. Potential of agricultural by-product-based activated carbons for use in raw sugar decolourisation. *J. Sci. Food Agric.* **1997**, *75* (1), 117–124. https://doi.org/10.1002/(SICI)1097-0010(199709)75:1<117::AID-JSFA850>3.0.CO;2-M

Al-Wabel, M. I.; Al-Omran, A.; El-Naggar, A. H.; Nadeem, M.; Usman, A. R. A. Pyrolysis temperature induced changes in characteristics and chemical composition of biochar produced from conocarpus wastes. *Bioresour. Technol.* **2013**, *131*, 374–379. https://doi.org/10.1016/j.biortech.2012.12.165

Anastopoulos, I.; Katsouromalli, A.; Pashalidis, I. Oxidized biochar obtained from pine needles as novel adsorbent to remove caffeine from aqueous solutions. *J. Mol. Liq.* **2020**, *304*, 112661. https://doi.org/10.1016/j.molliq.2020.112661

Becker, H.; Matos, R. F.; Souza, J. A.; Lima D. A.; Souza, T. C.; Longhinotti, E. Pseudo-stem banana fibers: Characterization and chromium removal. *Orbital: Electon.* J. *Chem.* **2013**, *5* (3), 164–170.

Binh, Q. A.; Nguyen, H.-H. Investigation the isotherm and kinetics of adsorption mechanism of herbicide 2,4-dichlorophenoxyacetic acid (2,4-D) on corn cob biochar. *Bioresor. Technol. Rep.* **2020**, *11*, 100520. https://doi.org/10.1016/j.biteb.2020.100520

Buehrle, D. J.; Wagener, M. M.; Clancy, C. J. Outpatient Fluoroquinolone Prescription Fills in the United States, 2014 to 2020: Assessing the Impact of Food and Drug Administration Safety Warnings. *Antimicrob. Agents Chemotherapy* **2021**, *65* (7), e00151-21. https://doi.org/10.1128/AAC.00151-21

Buerge, I. J.; Poiger, T.; Müller, M. D.; Buser, H.-R. Caffeine, an Anthropogenic Marker for Wastewater Contamination of Surface Waters. *Environ. Sci. Technol.* **2003**, *37* (4), 691–700. https://doi.org/10.1021/es020125z

Brazil. Ministry of Agriculture, Livestock and Supply. National Supply Company – CONAB. Acompanhamento da safra brasileira de cana-de-açúcar: v.7 - Safra 2020/21 n.4 - Quarto levantamento, 2021; pp 15. Available in: http://www.conab.gov.br (accessed 2021-07-04).

Chen, J.; Zhang, D.; Zhang, H.; Ghosh, S.; Pan, B. Fast and slow adsorption of carbamazepine on biochar as affected by carbon structure and mineral composition. *Sci. Total Environ.* **2017**, *579*, 598–605. https://doi.org/10.1016/j.scitotenv.2016.11.052

Chen, W.-H.; Hsu, H.-J.; Kumar, G.; Budzianowski, W. M.; Ong, H. C. Predictions of biochar production and torrefaction performance from sugarcane bagasse using interpolation and regression analysis. *Bioresour. Technol.* **2017**, 246, 12–19. https://doi.org/10.1016/j.biortech.2017.07.184

Correa-Navarro, Y. M.; Giraldo, L.; Moreno-Piraján, J. C. Biochar from fique bagasse for remotion of caffeine and diclofenac from aqueous solution. *Molecules* **2020**, *25* (8), 1849. https://doi.org/10.3390/molecules25081849

Dias, D. S.; Crespi, M. S.; Torquato, L. D. M.; Kobelnik, M.; Ribeiro, C. A. Torrefied banana tree fiber pellets having embedded urea for agricultural use. *J. Therm. Anal. Calorim.* **2018,** *131*, 705–712. https://doi.org/10.1007/s10973-016-6049-7

Granados, D. A.; Ruiz, R. A.; Vega, L. Y.; Chejne, F. Study of reactivity reduction in sugarcane bagasse as consequence

of a torrefaction process. *Energy* **2017**, *139*, 818–827. https://doi.org/10.1016/j.energy.2017.08.013

Hafshejani, L. D.; Hooshmand, A.; Naseri, A. A.; Mohammadi, A. S.; Abbasi, F.; Bhatnagar, A. Removal of nitrate from aqueous solution by modified sugarcane bagasse biochar. *Ecol. Eng.* **2016**, *95*, 101–111. https://doi.org/10.1016/j.ecoleng.2016.06.035

Huang, W.; Chen, J.; Zhang, J. Removal of ciprofloxacin from aqueous solution by rabbit manure biochar. *Environ. Technol.* **2020**, *41* (11), 1380–1390. https://doi.org/10.1080/09593330.2018.1535628

Ibrahim, R. H. H.; Darvell, L. I.; Jones, J. M.; Williams, A. Physicochemical characterization of torrefied biomass. *J. Anal. Appl. Pyrolysis* **2013**, *103*, 21–30. https://doi.org/10.1016/j.jaap.2012.10.004

International Biochar Initiative. S*tandardized Product Definition and Product Testing Guidelines for Biochar That Is Used in Soil* 2.1, 2015; 61. https://www.biochar-international.org/wp-content/uploads/2018/04/IBI_Biochar_Standards_V2.1_Final.pdf (accessed 2022-03-23).

Inyang, M.; Dickenson, E. The potential role of biochar in the removal of organic and microbial contaminants from potable and reuse water: A review. *Chemosphere* **2015**, *134*, 232–240. https://doi.org/10.1016/j.chemosphere.2015.03.072

Jayaraman, K.; Gokalp, I.; Petrus, S.; Belandria, V.; Bostyn, S. Energy recovery analysis from sugar cane bagasse pyrolysis and gasification using thermogravimetry, mass spectrometry and kinetic models. *J. Anal. Appl. Pyrolysis* **2018**, *132*, 225–236. https://doi.org/10.1016/j.jaap.2018.02.003

Keiluweit, M.; Kleber, M. Molecular-Level Interactions in Soils and Sediments: The Role of Aromatic π-Systems. *Environ. Sci. Technol.* **2009**, *43* (10), 3421–3429. https://doi.org/10.1021/es8033044

Li, L.; Yang, M.; Lu, Q.; Zhu, W.; Ma, H.; Dai, L. Oxygen-rich biochar from torrefaction: A versatile adsorbent for water pollution control. *Bioresour. Technol.* **2019**, *294*, 122142. https://doi.org/10.1016/j.biortech.2019.122142

Li, Z.; Wang, Z.; Wu, X.; Li, M.; Liu, X. Competitive adsorption of tylosin, sulfamethoxazole and Cu(II) on nano-hydroxyapatitemodified biochar in water. *Chemosphere* **2020**, *240*, 124884. https://doi.org/10.1016/j.chemosphere.2019.124884

Liang, L.; Xi, F.; Tan, W.; Meng, X.; Hu, B.; Wang, X. Review of organic and inorganic pollutants removal by biochar and biochar-based composites. *Biochar* **2021**, *3*, 255–281. https://doi.org/10.1007/s42773-021-00101-6

Liu, X.; Liao, J.; Song, H.; Yang, Y.; Guan, C.; Zhang, Z. A Biochar-Based Route for Environmentally Friendly Controlled Release of Nitrogen: Urea-Loaded Biochar and Bentonite Composite. *Sci. Rep.* **2019**, *9*, 9548. https://doi.org/10.1038/s41598-019-46065-3

Ma, S.; Si, Y.; Wang, F.; Su, L.; Xia, C.; Yao, J.; Chen, H.; Liu, X. Interaction processes of ciprofloxacin with graphene oxide and reduced graphene oxide in the presence of montmorillonite in simulated gastrointestinal fluids. *Sci. Rep.* **2017**, *7*, 2588. https://doi.org/10.1038/s41598-017-02620-4

Marasco Júnior, C. A.; Luchiari, N. C.; Lima Gomes, P. C. F. Occurrence of caffeine in wastewater and sewage and applied techniques for analysis: a review. *Eclética Quím. J.* **2019**, *44* (4), 11–26. https://doi.org/10.26850/1678-4618eqj.v44.4.2019.p11-26

Marasco Júnior, C. A.; Silva, B. F.; Lamarca, R. S.; Lima Gomes, P. C. F. Automated method to determine pharmaceutical compounds in wastewater using on-line solid-phase extraction coupled to LC-MS/MS. *Anal. Bional. Chem.* **2021**, *413*, 5147–5160. https://doi.org/10.1007/s00216-021-03481-7

Mohanty, S. K.; Valenca, R.; Berger, A. W.; Yu, I. K. M.; Xiong, X.; Saunders, T. M.; Tsang, D. C. W. Plenty of room for carbon on the ground: Potential applications of biochar for stormwater treatment. *Sci. Total Environ.* **2018**, *625*, 1644–1658. https://doi.org/10.1016/j.scitotenv.2018.01.037

Morais, L. C.; Maia, A. A. D.; Guandique, M. E. G.; Rosa, A. H. Pyrolysis and combustion of sugarcane bagasse. *J. Therm. Anal. Calorim.* **2017**, *129*, 1813–1822. https://doi.org/10.1007/s10973-017-6329-x

Mubarik, S.; Saeed, A.; Athar, M. M.; Iqbal, M. Characterization and mechanism of the adsorptive removal of 2,4,6-trichlorophenol by biochar prepared from sugarcane baggase. *J. Ind. Eng. Chem.* **2015**, *33*, 115–121. https://doi.org/10.1016/j.jiec.2015.09.029

Oliveira, F. R.; Patel, A. K.; Jaisi, D. P.; Adhikari, S.; Lu, H.; Khanal, S. K. Environmental application of biochar: Current status and perspectives. *Bioresour. Technol.* **2017**, *246*, 110–122. https://doi.org/10.1016/j.biortech.2017.08.122

Osińska, A.; Harnisz, M.; Korzeniewska, E. Prevalence of plasmid-mediated multidrug resistance determinants in fluoroquinolone-resistant bacteria isolated from sewage and surface water. *Environ. Sci. Pollut. Res.* **2016**, *23*, 10818–10831. https://doi.org/10.1007/s11356-016-6221-4

Osonwa, U. E.; Ugochukwu, J. I.; Ajaegbu, E. E.; Chukwu, K. I.; Azevedo, R. B.; Esimone, C. O. Enhancement of antibacterial activity of ciprofloxacin hydrochloride by complexation with sodium cholate. *Bull. Fac. Pharm. Cairo Univ.* **2017**, *55* (2), 233–237. https://doi.org/10.1016/j.bfopcu.2017.09.006

Pendolino, F. Self-assembly of molecules on nanostructured graphene. Ph.D. Dissertation, Universidad Autónoma de Madrid, Madrid, Spain, 2014.

Quéno, L. R. M.; Souza, A. N.; Costa, A. F.; Valle, A. T.; Joaquim, M. S. Aspectos técnicos da produção de *pellets* de madeira. *Ciênc. Florest.* **2019**, *29* (3), 1478–1489. https://doi.org/10.5902/1980509820606

Ramos, S. N. C.; Xavier, A. L. P.; Teodoro, F. S.; Gil, L. F.; Gurgel, L. V. A. Removal of cobalt(II), copper(II), and nickel(II) ions from aqueous solutions using phthalate-functionalized sugarcane bagasse: Mono- and multicomponent adsorption in batch mode. *Ind. Crops Prod.* **2016**, *79*, 116–130. https://doi.org/10.1016/j.indcrop.2015.10.035

Rangabhashiyam, S.; Balasubramanian, P. The potential of lignocellulosic biomass precursors for biochar production: Performance, mechanism and wastewater application—A review. *Ind. Crops Prod.* **2019**, *128*, 405–423. https://doi.org/10.1016/j.indcrop.2018.11.041

Regalbuto, J. R.; Robles, J. O. The engineering of Pt/Carbon catalyst preparation: for application on Proton Exchange Fuel Cell Membrane (PEFCM). Progress Report, University of Illinois, Chicago, USA, 2004. https://amrel.bioe.uic.edu/NSFREU2004/Reports2004/Jaime%20Robles_Final%20Report.pdf (accessed 2022-03-23)

Rodríguez-Díaz, J. M.; García, J. O. P.; Sánchez, L. R. B.; Silva, M. G. C.; Silva, V. L.; Arteaga-Pérez, L. E. Comprehensive Characterization of Sugarcane Bagasse Ash for Its Use as an Adsorbent. *BioEnergy Res.* **2015**, *8*, 1885–1895. https://doi.org/10.1007/s12155-015-9646-6

SciFinder – ACS Solutions. Available in: https://scifinder.cas.org (accessed 2021-06-18).

Sun, J.; Sakai, S.; Tauchi, Y.; Deguchi, Y.; Chen, J.; Zhang, R.; Morimot, K. Determination of lipophilicity of two quinolone antibacterials, ciprofloxacin and grepafloxacin, in the protonation equilibrium. *Eur. J. Pharm. Biopharm.* **2002**, *54* (1), 51–58. https://doi.org/10.1016/S0939-6411(02)00018-8

Sun, L.; Chen, D.; Wan, S.; Yu, Z. Adsorption studies of dimetridazole and metronidazole onto biochar derived from sugarcane bagasse: Kinetic, equilibrium, and mechanisms. *J. Polym. Environ.* **2018**, *26*, 765–777. https://doi.org/10.1007/s10924-017-0986-5

Tag, A. T.; Duman, G.; Uçar, S.; Yanik, J. Effects of feedstock type and pyrolysis temperature on potential applications of biochar. *J. Anal. Appl. Pyrolysis.* **2016**, *120*, 200–206. https://doi.org/10.1016/j.jaap.2016.05.006

Tan, X.; Liu, Y.; Zeng, G.; Wang, X.; Hu, X.; Gu, Y.; Yang, Z. Application of biochar for the removal of pollutants from aqueous solutions. *Chemosphere* **2015**, *125*, 70–85. https://doi.org/10.1016/j.chemosphere.2014.12.058

Torquato, L. D. M.; Crnkovic, P. M.; Ribeiro, C. A.; Crespi, M. S. New approach for proximate analysis by thermogravimetry using CO_2 atmosphere: Validation and application to different biomasses. *J. Therm. Anal. Calorim.* **2017**, *128*, 1–14. https://doi.org/10.1007/s10973-016-5882-z

Tran, H. N.; You, S.-J.; Hosseini-Bandegharaei, A.; Chao, H.-P. Mistakes and inconsistencies regarding adsorption of contaminants from aqueous solutions: A critical review. *Water Res.* **2017**, *120*, 88–116. https://doi.org/10.1016/j.watres.2017.04.014

Tumuluru, J. S.; Sokhansanj, S.; Hess, J. R.; Wright, C. T.; Boardman, R. D. A review on biomass torrefaction process and product properties for energy applications. *Ind. Biotechnol.* **2011**, *7* (5), 384–401. https://doi.org/10.1089/ind.2011.7.384

Wang, B.; Jiang, Y.; Li, F.; Yang, D. Preparation of biochar by simultaneous carbonization, magnetization and activation for norfloxacin removal in water. *Bioresour. Technol.* **2017**, *233*, 159–165. https://doi.org/10.1016/j.biortech.2017.02.103

Yi, K.; Wang, D.; QiYang, Li, X.; Chen, H.; Sun, J.; An, H.; Wang, L.; Deng, Y.; Liu, J.; Zeng, G. Effect of ciprofloxacin on biological nitrogen and phosphorus removal from wastewater. *Sci. Total Environ.* **2017**, *605–606*, 368–375. https://doi.org/10.1016/j.scitotenv.2017.06.215

Yuan, J.-H.; Xu, R.-K.; Zhan, H. The forms of alkalis in the biochar produced from crop residues at different temperatures. *Bioresour. Technol.* **2011**, *102* (3), 3488–3497. https://doi.org/10.1016/j.biortech.2010.11.018